

# Equatorial plasma bubbles observed in large longitudinal range during a magnetic storm on 5 April 2006

*Guanyi Ma<sup>\*1</sup>, Jinghua Li<sup>1</sup>, Takashi Maruyama<sup>2</sup>, Shuli Song<sup>3</sup>, and Junshen Xue<sup>3</sup>*

<sup>1</sup> National Astronomical Observatories, Chinese Academy of Sciences, Beijing 100012, China,  
guanyima@nao.cas.cn

<sup>2</sup> National Institute of Information and Communications Technology, Tokyo 184-8795, Japan,  
tmaru@nict.go.jp

<sup>3</sup> Shanghai Astronomical Observatory, Chinese Academy of Sciences, Shanghai 200030, China,  
slsong@shao.ac.cn

## Abstract

During magnetic storms, energy injection at high latitudes results in highly disturbed electric fields and thermospheric winds to dominate the low latitude and equatorial ionosphere. This makes a significant difference of the stormtime equatorial plasma bubbles from those in quiet time ionosphere. This paper presents plasma bubbles observed with 51 dual-frequency GPS receivers during the main phase of a medium magnetic storm on 5 April 2006. With the rate of the total electron content index (ROTI) maps, the plasma bubbles were found between 90°E and 160°E in longitude, 12°S and 33°N in latitude. It is the first time to observe bubbles in such an unusually large longitude range with ground-based GPS receivers. The plasma bubbles displayed asymmetry in north-south hemisphere. The bubbles in the southern hemisphere appeared ~1 h after sunset and survived ~9 h. Those in the northern hemisphere appeared ~1.5 h after sunset and survived ~4 h.

## 1. Introduction

Equatorial plasma bubble refers to the low density plasma region in the nighttime equatorial ionosphere that contains strong irregularities. They develop in the bottom side of the F region where the generalized Rayleigh-Taylor instability driven by the gravitational force and eastward electric field operates [1-2]. During magnetic storms, energy injection at high latitudes results in highly disturbed electric fields and thermospheric winds to dominate the low latitude and equatorial ionosphere. This makes a significant difference of the stormtime equatorial plasma bubbles from those in quiet time ionosphere. Moreover, the characteristics of the EPBs are different for different magnetic storms [3].

Since the civilian use of the Global Positioning System (GPS) was enabled, the ionospheric TEC can be measured with dual frequency GPS receivers economically and effectively. The principle is based on the frequency dependence of the refractive index of radio waves in the ionospheric plasma. With the ground-based GPS receivers and hence networks being increasingly set up worldwide, characteristics of the ionosphere can be studied extensively with TEC in large regional or global scale. Utilizing the rate of change of the TEC, termed ROT, and further, a rate of TEC index (ROTI), several researchers studied the evolution of large scale irregularities during magnetic storms at both low and high latitudes [4-5].

This paper presents a case of equatorial plasma bubbles in an unusually large longitudinal range from eastern Indian Ocean to western Pacific Ocean between  $90^{\circ}\sim 160^{\circ}\text{E}$  observed with GPS receivers during a magnetic storm on Apr. 5 2006. The data was from 51 GPS receivers located between  $70^{\circ}\text{E}$  and  $310^{\circ}\text{E}$  in longitude,  $20^{\circ}\text{S}$  and  $40^{\circ}\text{N}$  in latitude. Figure 1 shows the locations of the GPS receivers. The relative TECsll along line of sight was first obtained from the differential phase at 30-s intervals. Then ROT was determined by taking the difference between the TECsll at two successive times. ROTI is defined by the standard deviation of ROT,  $\text{ROTI} = \sqrt{\langle \text{ROT}^2 \rangle - \langle \text{ROT} \rangle^2}$  for each 5-min interval [1]. ROTI map was made by projecting the ROTI values on the Earth from the ionospheric piercing point at 400 km altitude.

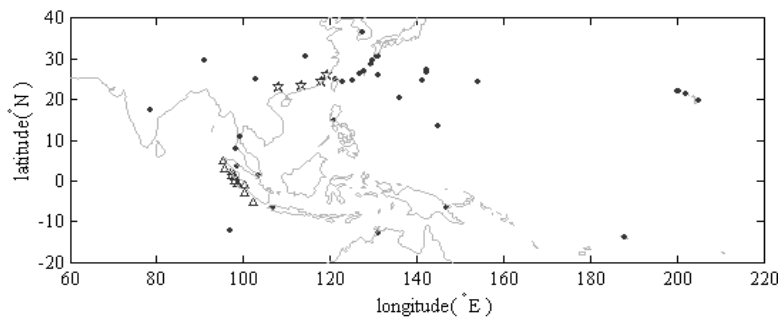


Fig. 1. Geographic locations of GPS observation sites. Different symbols distinguish receivers from different networks.

## 2. The magnetic storm on 5 April 2006

The magnetic storm commenced at about 0800 UT 4 April 2006, as shown in Fig. 2. This is a medium scale storm. With the abrupt turning of the IMF Bz from northward to southward, the Dst index started to decrease until -87 nT at about 1500 UT on 5 April 2006. Then the IMF Bz turned northward and the Dst started to increase, indicating the storm entered the recovery phase.

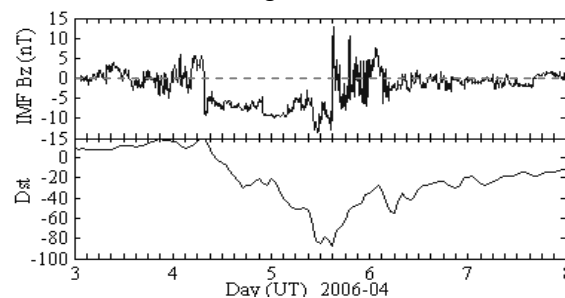


Fig. 2. IMF Bz and geomagnetic indices during 3-8 April 2006. IMF Bz was plotted with a time delay of 80 min to account for the propagation of the solar wind at the measured speed of  $\sim 300\text{m/s}$ .

## 3. Results from GPS observation

Figure 3 shows slant TEC and ROTI variations with time at two observation sites in northern and southern hemispheres, respectively. TEC depletion and large ROTI values can be observed after 1000 UT. Irregularities were first observed at LAEL ( $147.0^{\circ}\text{E}$ ,  $6.7^{\circ}\text{S}$ ) in southern hemisphere at  $\sim 1000$  UT (1900 LT) on 5 April 2006. Sunset was 1800 LT. So the irregularities appeared  $\sim 1$  hour after the sunset. In northern hemisphere irregularities were first observed at TWTF ( $121.2^{\circ}\text{E}$ ,  $25.0^{\circ}\text{N}$ ) at  $\sim 1130$  UT

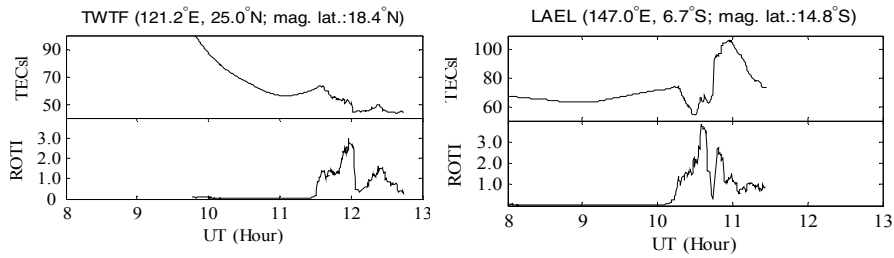


Fig. 3. Manifested as TEC depletions, plasma bubbles observed at two sites. (1930 LT) on the same day. They appeared  $\sim 1.5$  h after the sunset.

The plasma bubbles in northern hemisphere started to decay at  $\sim 1400$ - $1430$  UT and disappeared one hour later at  $\sim 1530$  UT, although appeared later than those at southern hemisphere. The bubbles in southern hemisphere began to decay at  $\sim 1700$  UT and disappeared two hours later at 1900 UT. The bubbles in the southern hemisphere survived  $\sim 9$  h. Those in the northern hemisphere survived  $\sim 4$  h. Fig. 4 shows the spatial distribution of the irregularities between  $90$ - $160$  E in longitude, and  $12$  S- $33$  N in latitude. In this region, the magnetic equator is at  $\sim 7.9$  N. It should be noted that these irregularities occupied an unusually large longitudinal range  $70^\circ$  and extended asymmetrically in north-south hemisphere covering a latitude range of  $45^\circ$ .

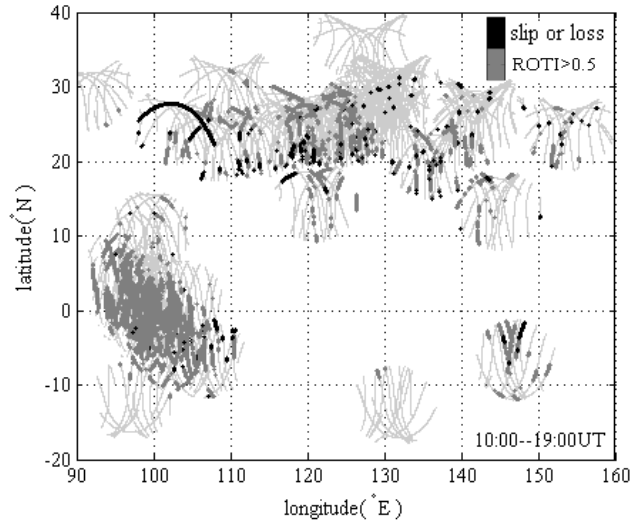


Fig. 4. Spatial distribution of the plasma bubbles between 10:00 and 19:00 UT. Cycle slip and loss of lock are also used to indicate the existence of irregularities.

To further understand the whole picture of the plasma bubbles during the storm, the difference between the TECs on 5 and 4 April 2006 at Fuzhou ( $119.3^\circ$ E,  $26.0^\circ$ N) is shown in Fig. 5 as an example. It

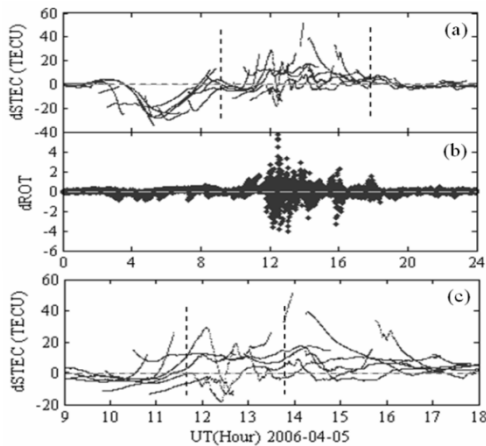


Fig. 5. Changes of slant TECs at Fuzhou ( $119.3^\circ$ E,  $26.0^\circ$ N, mag.Lat.  $19.6^\circ$ N) during the storm time compared with those in quiet ionosphere.

indicates from the top and middle panels that before the plasma bubbles appeared a negative ionospheric storm during 0300-0800 UT on 5 April 2006. The bottom panel is the amplification of the TEC difference covering the bubble existence duration of 1130-1700 UT. When the plasma bubbles were observed, the TEC was enhanced. This indicates that the ionosphere was probably uplifted. The uplifting of the ionosphere can be explained in terms of electric fields or thermospheric winds resulted from energy injection at high latitudes during the magnetic storm. Moreover, are these bubbles originated from the same source? With only the GPS observations, the generation of the plasma bubbles in this paper cannot be clarified.

#### 4. Summary

With 51 dual-frequency GPS receivers ionospheric plasma bubbles were observed in a large longitude range during the main phase of a medium magnetic storm on 5 April 2006. The GPS receivers are located between 70 E and 310 E in longitude, 20 S and 40 N in latitude. With the ROTI maps, the plasma bubbles were found between 90 E and 160 E in longitude, 12 S and 33 N in latitude. It should be noted that these bubbles occupied an unusually large longitudinal extension. The accompanying event with the bubbles was a negative ionospheric storm happened earlier. The plasma bubbles displayed asymmetry in north-south hemisphere. The plasma bubbles appeared earlier and survived longer in the southern hemisphere than those in the northern hemisphere. The bubbles in the southern hemisphere appeared  $\sim 1$  h after sunset and survived  $\sim 9$  h. Those in the northern hemisphere appeared  $\sim 1.5$  h after sunset and survived  $\sim 4$  h. With only the GPS data, the generation of the plasma bubbles in this paper cannot be clarified. Multi-instrumental observation data is needed and anticipated to study these plasma bubbles in detail.

#### 5. References

1. R. F. Woodman and L. H. CÉSAR, "Radar observations of F region equatorial irregularities", *J. Geophys. Res.*, 1976, 81(31): 5447-5466.
2. S. Basu, K. M. Groves, J. M. Quinn, P. Doherty, "A comparison of TEC fluctuations and scintillations at Ascension Island", *J. Atmos. and solar-Terr. Phys.*, 1999, 61:1219-1226.
3. M. A. Abdu, "Equatorial spread F/plasma bubble irregularities under storm time disturbance electric fields", *J. Atmos. and solar-Terr. Phys.*, 2012, 75-76:44-56.
4. X. Pi, A. J. Mannucci, U. J. Lindqwister, and C. M. Ho, "Monitoring of global ionospheric irregularities using the worldwide GPS network", *Geophys. Res. Lett.*, 1997, 24:2283-2486.
5. J. P. McClure, W. B. Hanson, and J. H. Hoffman, "Plasma bubbles and irregularities in the equatorial ionosphere", *J. Geophys. Res.*, 1977, 82:2650-2656.